

# Application of Self-Healing Materials to Leak Repair in Inflatable Structures



AE 8900 MS Special Problems Report  
Space Systems Design Lab (SSDL)  
Guggenheim School of Aerospace Engineering  
Georgia Institute of Technology  
Atlanta, GA

Author:  
Emily Erin Simmons

Advisor:  
Prof. Brian C. Gunter

May 3, 2019

# Application of Self-Healing Materials to Leak Repair in Inflatable Space Structures

Emily Simmons<sup>1</sup>

*Georgia Institute of Technology, Atlanta, Georgia, 30332, USA*

As the duration of crewed spaceflight missions increases, so does the need for habitable volume. Inflatable structures have been proposed as one solution, but they face challenges in terms of their resilience and repair of leaks. This study examines the use of self-healing materials as a method to repair damage to the inflatable structures, without any human intervention. The study used the finite element analysis software Abaqus to evaluate the effects of thickness, crack size, and initial stresses on the healing efficiency of both microvascular and microencapsulated self-healing materials. The analysis showed that cracks up to 0.2 mm can be healed effectively for the materials explored; however, the healing requires a significant increase in necessary volume of healing agent over the nominal, unloaded case. As a result, the microvascular system is considered to be superior to the microencapsulation method for use in inflatable structures, as it can deliver a continuous supply of the healing agent.

## I. Nomenclature

$a$	=	maximum width of cut
$C_f$	=	coefficient of friction
$c_0$	=	bulk speed of sound
$E$	=	Young's modulus
$FEA$	=	finite element analysis
$FEM$	=	finite element modelling
$p$	=	pressure
$R$	=	specific gas constant
$Re$	=	Reynold's number
$s$	=	linear Hugoniot slope coefficient
$T$	=	temperature
$t$	=	total thickness of material
$t_f$	=	equivalent thickness of healing agent
$V_l$	=	volume of healing agent that is lost
$V_o$	=	nominal volume required to heal
$v$	=	velocity
$v_f$	=	volume fraction of healing agent
$\Gamma$	=	Grüneisen parameter
$\delta_i$	=	maximum transverse deflection of inner face of healing agent
$\delta_o$	=	maximum transverse deflection of outer face of healing agent
$\mu$	=	dynamic viscosity
$\rho$	=	density

## II. Introduction

As humans spend longer and longer periods in space, there are growing concerns regarding the minimal livable volume for the astronauts using current technologies. One proposed solution is the use of inflatable structures, which allow a significant increase in volume with a much lower mass. However, inflatable structures pose new challenges, such as the identification and repair of leaks. Most proposed designs for inflatable habitats call for the use of multiple

---

<sup>1</sup> Graduate Student, Aerospace Engineering.

layers, including, at a minimum, a bladder layer, a structural restraint layer, and a protective layer, with thermal insulation and radiation shielding being incorporated either as additional layers or incorporated into existing layers [1]. The bladder layer is responsible for maintaining the pressure seal, sometimes using multiple layers which may be sandwiched between other layers [2]. One such proposed design comes from TransHab and is shown in Fig. 1 below (taken from [2]). In this example, multiple bladder layers are sandwiched between a scuff layer and a restraint layer.

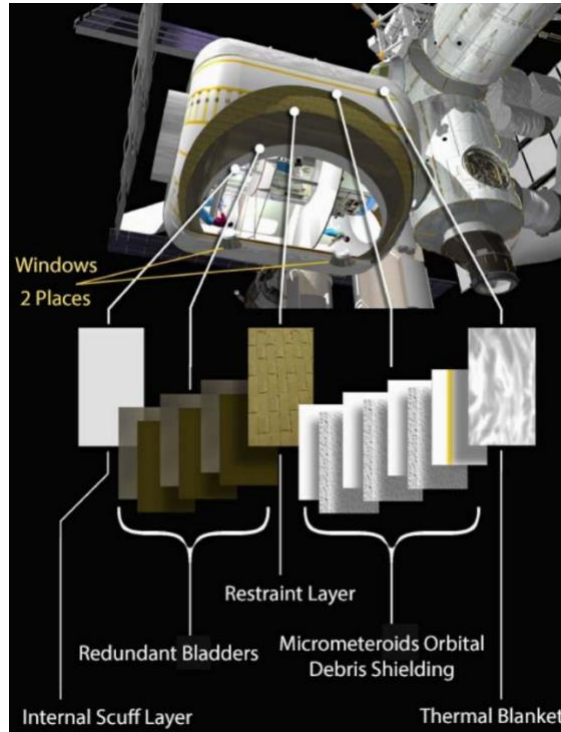


**Fig. 1 Proposed TransHab layer buildup [2].**

As the bladder layer is the sole protection against pressure loss, any holes or fractures, regardless of size, are a critical safety concern. However, locating and repairing the holes is difficult due to the inaccessible nature of the bladder layer. In this paper, self-healing materials are proposed as a potential solution to inspection and repair problems, as they can repair leaks without human identification or intervention. While many studies have been performed to determine the properties of self-healing materials, such as Brown, Sottos, and White [3], who performed fracture testing or Wang, et al. [4], who evaluated the elasticity of a self-healing elastomer, few have addressed their ability to seal a leak in a pressure vessel, and minimal studies have considered them for use in a space environment. To explore this, this study analyzes self-healing materials using the microencapsulation or microvascular methods using the FEA software Abaqus<sup>2</sup> to determine their capability to heal while under pressure loading. In addition, a survey of current self-healing materials is performed in order to identify candidates for use. While the author would like to run physical tests, due to time and budget constraints on the study, the tests are infeasible.

The study showed that narrow cracks could heal easily, up to 0.2 mm wide (before stretching). However, the healing requires a significant increase in necessary volume of healing agent over the nominal, unloaded case. As a result, the microvascular system is considered to be superior to the microencapsulation method for use in inflatable structures, as it can deliver a continuous supply of the healing agent. After healing, the Von Mises stress in the material is shown to increase by a factor of 2.89 to 3.45, but even with the increase, the stress remains well below the yield strength of the material.

### III. Background

Multiple methods have been proposed to identify damage to inflatable structures. Alena, et al. [5], proposed a series of strain sensors to be placed around the capsule to identify volume reductions. Another group identified the

<sup>2</sup> <https://www.3ds.com/products-services/simulia/products/abaqus/>

potential to use electromagnetic sensors to locate damage [6]. However, both these methods are active processes, and neither addresses the repair of any damage. As many proposed designs for inflatable structures include multiple layers, the bladder layer is not necessarily accessible for repairs [6]. Self-healing materials are a potential alternative solution, which, with the proper implementation, could maintain and repair the pressure seal without the use of any active systems. These materials have already been investigated for use in airplanes; however, the materials investigated were rigid, while an inflatable structure requires flexible materials [7]. Self-healing materials come in two main types: non-autonomic and autonomic. Non-autonomic processes require an additional energy input, such as heat, whereas autonomic processes require nothing additional [8]. While the non-autonomic processes can be designed to be passive, such as by using the heat of hypervelocity impacts as the additional energy source (as temperatures can exceed 2500 K), the autonomic processes are intrinsically passive and will be the focus of this paper [9]. Self-healing materials can also be divided by the type of healing: intrinsic and extrinsic. Intrinsic healing uses chemical bonding and physical interaction between the crack surfaces, while extrinsic has a healing agent embedded in the material that is released upon crack formation. Intrinsic methods cannot always be used and tend to be non-autonomic, but extrinsic methods tend to reduce the strength of the parent material [8]. While both types have drawbacks, this paper will focus on extrinsic, autonomic processes, as the goal is to show a system for repair which does not require human intervention. An example of an intrinsic, autonomic self-healing elastomer was developed by Wang, et al., with properties comparable to rubber [4]. There has been some research into the use of self-healing materials in space, including one brief study done to extend the design work for TransHab in 2006 [10]. However, as self-healing materials are still a relatively new technology, these early studies mainly serve as a baseline starting point to be developed and improved.

Analysis of inflatable structures and self-healing materials can be complex, due to high non-linearity and phase changes. However, numerous methods have been developed to account for both situations. Basic FEM programs typically allow the user to choose between explicit and implicit nonlinear analyses. While explicit is computationally less expensive, the implicit method is more accurate for dealing with inflatable structures [11]. In order to reduce the computational power required for the deployment of inflatable structures, they can be treated as a series of control volumes, with mass flow enforced between the control volumes based on the pressure difference [11]. For the self-healing materials, three models are suggested. The first is a theoretical model to focus on one basic aspect of the self-healing material largely in terms of thermodynamics or continuum equations. The second employs FEM to expand upon and confirm the results of the first. Finally, the third, called the correlation method, uses previous similar simulations and adjusts them to fit the new data. It also involves considering biological processes and applying them to engineering solutions [10]. Combining the methods for self-healing materials and inflatable structures allows the analysis of inflatable structures made from self-healing materials.

## **IV. Mechanics of Self-Healing**

### **A. Microencapsulation**

In the microencapsulation method of self-healing, healing agents are sealed within a hard shell and then embedded within the matrix material. When a crack is initiated within the material, the shell breaks, and the healing agent leaks out. If the healing agent requires a catalyst to harden, the catalyst is also embedded within the matrix material in a similar manner to the healing agent. When the crack is initiated, the catalyst leaks out at the same time as the healing agent and the two mix, initiating the hardening of the healing agent. This process is shown below in Fig. 2 (taken from [12]).

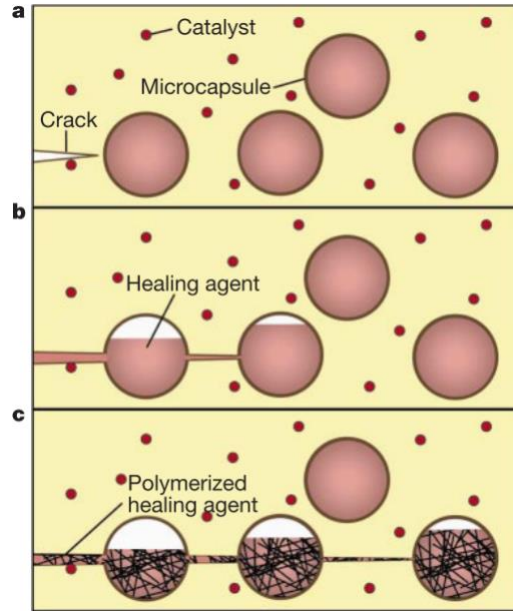


**Fig. 2 Microencapsulation healing process. a) Initial crack formation. b) Crack reaches microcapsules and is filled with healing agent. c) Healing agent mixes with catalyst and polymerizes [12].**

Microencapsulation is an explicit, non-autonomous healing process. It is the oldest method for self-healing and, as such, has been extensively studied [13]. However, it has the disadvantage that healing can only occur in any given location once [8]. In order to overcome this, a second method, microvascular system, discussed below, was introduced.

There have been many healing agents proposed for use in microcapsules. For self-healing materials, these agents tend to be monomers, such as epoxies and linseed oils [8]. While most healing agents currently researched require the catalyst, there are some proposed systems which do not require a catalyst, such as isophorone diisocyanate (IPDI) [13].

### **B. Microvascular System**

The microvascular system is similar to the microencapsulation method in that it releases a healing agent into the crack, but while the microencapsulation method is single use, the microvascular system can be used repeatedly. This is enabled by the delivery of healing agents through a system of tubes within the material. The healing agent is kept pressurized within the tubes, and, when a tube is broken, the healing agent leaks out into the crack. After healing, the tube refills with the healing agent so that it will again fill the crack the next time one occurs. Similarly, a catalyst can also be distributed throughout the material through a second microvascular system [14]. However, the microvascular system does reduce the strength of the matrix material significantly more than the microencapsulation method, and would not be good in situations requiring high strength [8]. The microvascular system can be easily applied with the same healing agents as the microencapsulation method.

## **V. Model Setup**

The study was performed using finite element analysis techniques and was run using the Abaqus software package. The geometry, loads, boundary conditions, and analysis type were set up in Abaqus' pre- and post-processor, Abaqus/CAE, while the analysis was run on a cluster, in order to improve runtime. Postprocessing of the results was again performed in Abaqus/CAE. Three separate models were created: one to model the healing process, and two to determine the increase in stress in the material after healing.

### **A. Simplifying Assumptions**

The model made a number of simplifying assumptions in order to reduce the model complexity and improve run time. First, the hole was assumed to be symmetric. Second, any turbulence of the flow through the hole is neglected. Under these two assumptions, the model can be created using symmetric constraints, reducing the model to a quarter

of its initial size. The area being modelled was considered to be small enough relative to the circumference of the pressure vessel that it could be modelled as a flat plate instead of a curved shell. Rather than model the random distribution of microcapsules or microvascular systems, which would result in elements far smaller than the overall thickness of the material, the healing agent was assumed to be grouped in layers, but the overall volume fraction was maintained. The chemical interactions were not modelled; it was assumed that the material was designed well enough that they would take place and cause the polymerization of the healing agent. A constant temperature of 27°C was assumed, due to the bladder's proximity to the interior of the inflatable module.

### B. Geometry and Material

The first model represented the hole and was used to model the healing agent filling the crack. The hole was modelled as a cross cut, with a square surrounding the cut. The cut was assumed to have a length of 2 mm in each direction, with a maximum width,  $a$ , ranging from 0.08 mm to 1 mm. These hole sizes were chosen based on the studies performed by Cadogan, et al. [1], who references these sizes as being typical of bladders. The geometry is shown in Fig. 3 below.

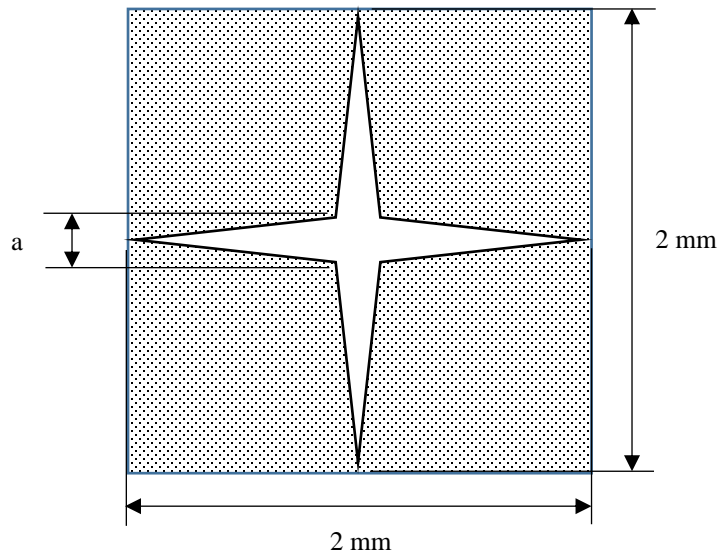


**Fig. 3 Cross cut geometry**

Due to symmetry, only one-quarter of the square was modelled. The study considered an overall thickness of the material of 0.5 mm and 1 mm. These values were again based on the work of Cadogan, et al. [1] for the same reasons.

The healing agent was modelled as 0.025 mm layers dispersed evenly. The number of layers was chosen such that the total thickness was the equivalent healing agent thickness, calculated from Eq. (1) below, with a volumetric fraction of 0.3.

$$t_f = v_f t \quad (1)$$

This setup is shown in Fig. 4 and Fig. 5 below, where the tan sections are the matrix, and the green sections are the healing agent. The rigid elements are hidden in Fig. 4 in order to show the layers.

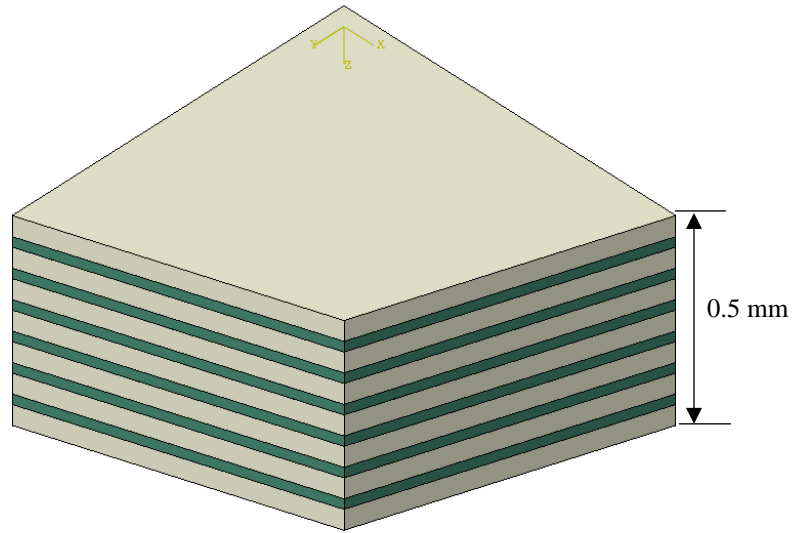


**Fig. 4 Isometric view of geometry of model of healing process.**

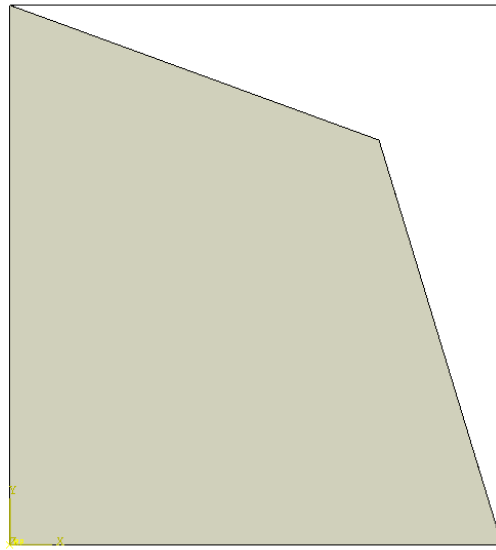


**Fig. 5 Top view of geometry of model of healing process.**

The matrix was modelled as a polyurethane film, with properties listed in Table 1 below.

**Table 1 Polyurethane material properties. [15]**

E	25 MPa
$\nu$	0.25
$\rho$	1.12 kg/m <sup>3</sup>
$\sigma_Y$	7.6 MPa

The healing agent was modelled as a viscous fluid using the Mie-Grüneisen equation of state using properties typical of liquid monomers. The exact properties are listed in Table 2 below.

**Table 2 Healing agent material properties. [16, 17]**

$\rho$	1.06 kg/m <sup>3</sup>
$\mu$	14 cP
$c_o$	2620 m/s
s	1.25
$\Gamma$	1.53

The second model represented the material after the crack had filled and the healing agent had catalyzed. It was modelled as a solid block, which tapered to 30% the total width on the faces of symmetry, beginning a distance of half the maximum crack width away from the face. This geometry is shown in Fig. 6 below. Figure 7 shows the full crack to demonstrate the connections along the crack tip.

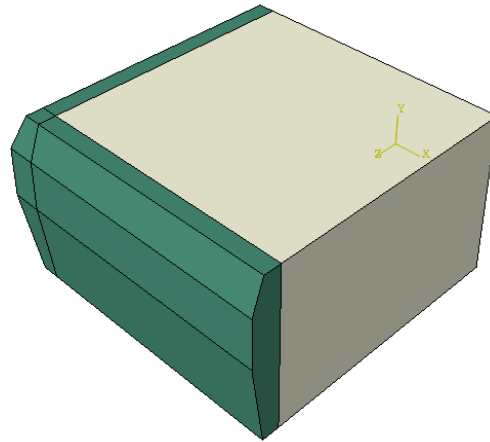


**Fig. 6 Geometry of second model.**

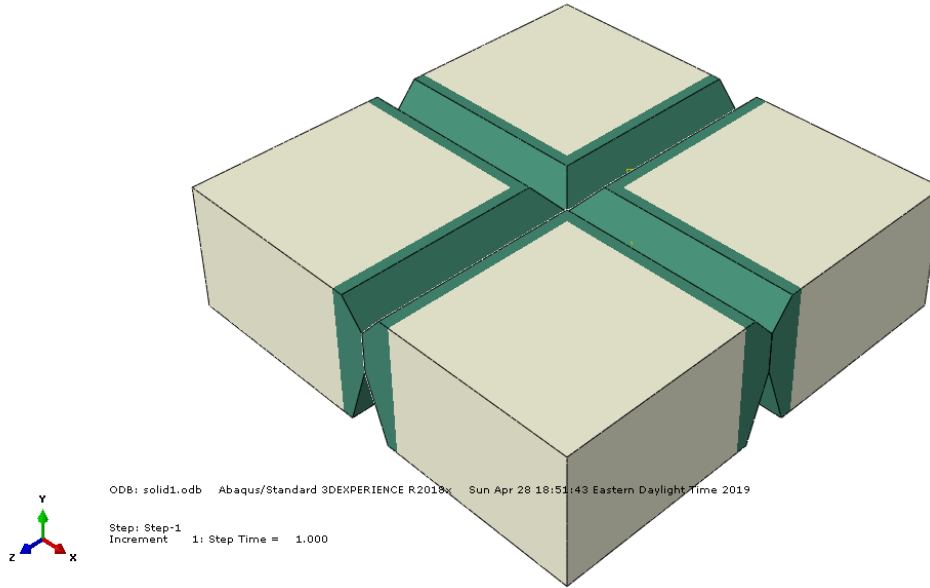


**Fig. 7 Assembled blocks displaying full crack geometry.**

The main portion of the block, the tan section, was modelled with a reduced Young’s modulus value of 17.5 MPa from the polyurethane in order to represent the healing agent and voids within the polyurethane matrix. The crack portion of the block, the green section, was modelled with the original polyurethane properties. This decision was made based on the use of polyurethane for the healing agent.

The third model represented the undamaged material, and was modelled as a cube, with the same overall dimensions as the first two. The entire model had the same reduced properties as the main portion of the previous model.

### C. Mesh

For the first model, both the matrix material and the healing agent were modelled using C3D8R elements, which are linear, reduced integration brick elements. The matrix was meshed to a global element size of 0.15 mm and the healing agent was meshed to a global element size of 0.1 mm. An analytical rigid surface was defined to enforce symmetry of the model, meshed with 0.5 mm rigid quadrilateral elements.

The second and third models were both modelled with C3D20R elements, which are quadratic, reduced integration brick elements. They were both meshed with a global element size of 0.05 mm, with local mesh seeds assigned to ensure three elements across the width of the crack portion.

### D. Boundary Conditions and Loading

The outer edges of the models were constrained using a pinned boundary condition. For the second and third models, the faces along the planes of symmetry were constrained using the symmetry boundary conditions. Loading conditions were applied based on the requirements set forth in NASA-STD-3001 [18]. As such, a uniform pressure force of 103 kPa, the maximum allowable pressure within the vehicle, was applied to one face of the plate. This pressure was chosen to simulate the worst-case scenario on the hole, assuming vacuum outside the bladder. Using the Beryline method, the velocity of the air escaping through the hole can be given as [19]:

$$v = \sqrt{\frac{2\Delta p}{\rho_{int}}} \quad (2)$$

Where  $\Delta p$  and  $\rho_{int}$  represent the change in pressure and internal air density, respectively. Applying the ideal gas law and noting that the difference in pressure is just the internal pressure, assuming that the exterior is large enough to remain in vacuum as the air exits, the velocity equation can be rewritten as:

$$v = \sqrt{2RT_{int}} \quad (3)$$

Assuming an internal temperature of 27°C, the maximum allowable value, the velocity was calculated as 415 m/s.

The stress exerted on the walls of the crack can be calculated as:

$$\tau = \frac{1}{2} \rho v^2 C_f = \Delta p C_f = \left( \frac{13.08}{\sqrt{a}} \right) [Pa] \quad (4)$$

Where  $a$  (the maximum cut width) is in meters and the coefficient of friction is given by the Blasius solution:

$$C_f = \frac{0.664}{\sqrt{Re}} = \frac{1.291 \cdot 10^{-4}}{\sqrt{a}} \quad (5)$$

The calculated shear stress is listed in Table 3 below.

**Table 3 Shear stresses on edges of crack due to air flow.**

a (mm)	$\tau$ (kPa)
0.08	1.462
0.2	0.925
0.5	0.585
0.7	0.494
1	0.414

In addition, an initial stress was applied to the healing agent, uniform in all directions. The effects of this initial stress were studied, with values ranging from 0 to 5 kPa.

## E. Analysis Setup

All analyses were run in Abaqus 2018. The analysis was divided into two segments. First, an explicit dynamic analysis was run to simulate the healing process, run for 0.1 seconds. This analysis was run using the first model. Next, a static step was run to determine the stresses of the undamaged and healed materials. This analysis was run using the second and third models. All the analyses were run with Nlgeom, or nonlinear geometry, enabled to account for the large displacements resulting from the highly elastic nature of polyurethane.

## VI. Results

### A. Healing Efficiency

The healing efficiency was studied in terms of the time for a crack to heal and the estimated material loss. The time to heal was determined by visual inspection of the model, determining when a full seal had been made along each of the planes of symmetry. The estimated material loss was determined by the percentage of layers which did not reach the planes of symmetry, and thus would not have sealed the hole. In addition, each result was marked as to whether the hole was completely sealed. For those without 100% material loss, a no response indicates that a small pinprick hole remained at the center. Due to the fidelity of the mesh, the results are unclear as to whether this small hole would be sealed or not, and additional study with a highly refined mesh or physical testing would be required. The results are listed in Table 4 below.

**Table 4 Healing efficiencies of different geometries.**

a (mm)	t (mm)	Initial Stress (kPa)	Stress	Time to Heal (s)	Estimated Material Loss	Complete Seal
0.08	1	0		0.005	0 %	Yes
0.2	1	0		0.085	16%	No
0.5	1	0		Inf	100 %	No
0.7	1	0		Inf	100 %	No
1	1	0		Inf	100 %	No
0.08	0.5	0		0.035	0 %	Yes
0.2	0.5	0		0.04	33 %	No
0.5	0.5	0		Inf	100 %	No
0.7	0.5	0		Inf	100 %	No
1	0.5	0		Inf	100 %	No
0.2	1	0.5		0.04	16 %	No
0.2	1	5		0.04	0 %	Yes
0.5	1	0.5		Inf	100 %	No
0.5	1	5		Inf	100 %	No

The materials that showed 100% material loss had a clear trend of the filler curving away from the planes of symmetry, and it was therefore determined that running the analysis for longer would not result in the sealing of the crack. An example of this phenomenon is shown in Fig. 8 below, with some of the rigid elements removed from the display for visualization purposes. While the healing agent does make some contact with the plane of symmetry, a large portion is pulled straight up, leaving a large portion of the crack still unsealed.

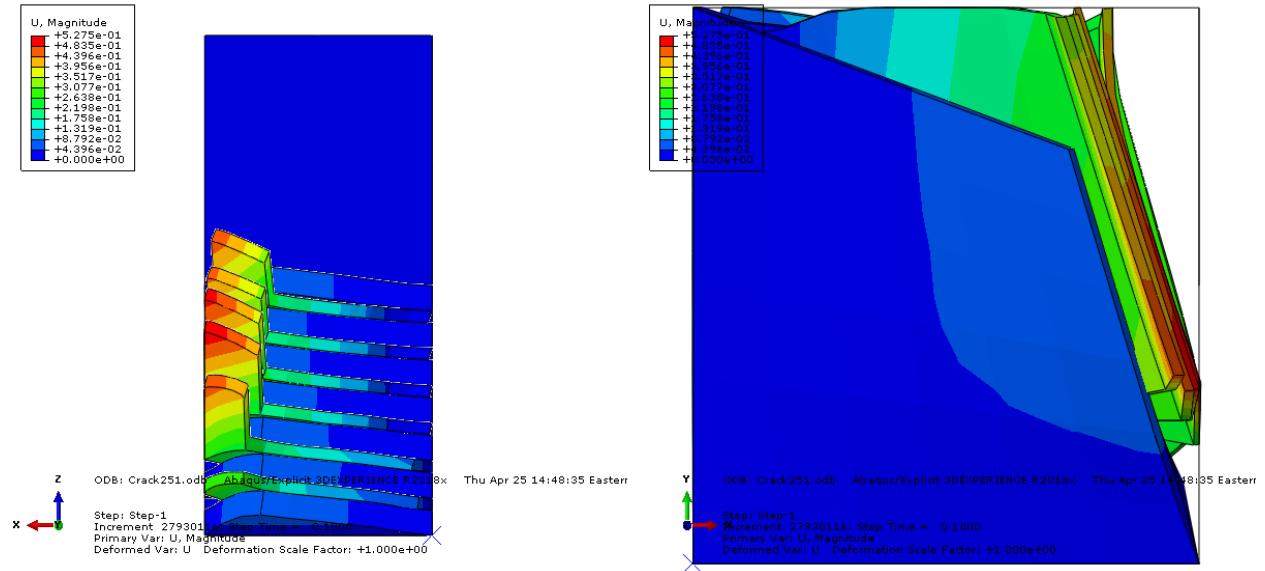


**Fig. 8 Deformation of part with 100% material loss. Left: Side view looking at cut face. Right: Top view looking at outside face of material.**

For the materials which sealed the crack, there was a definite correlation between increasing the thickness of the material and improvements in healing efficiency, both in time and in material loss. This result was verified with reference to Beiermann, et al. [20], who noticed similar trends in a three-layer composite material, with the center layer being a self-healing material. The trend in puncture size also matches to Beiermann’s work, as only the smaller punctures are able to heal. In addition, increasing the initial stress improved the material loss, but showed no effect on the time to heal.

## B. Deformation

The maximum deformation of the inner and outer faces of each test is recorded, and the estimated increase in volume of healing agent needed to seal the hole is calculated based on it using Eq. 6. This increase is the difference between the material extruding laterally across the hole versus the domed shape which results from the pressure load. The results are listed in Table 5 based on the maximum cut width and thickness of the modelled geometry.

$$\Delta V = 4 \left( \sqrt{\delta_i^2 + a^2} (t_f + \delta_o - \delta_i) \left( \frac{1}{1-V_l} \right) - at_f \right) \quad (6)$$

**Table 5 Maximum transverse deformation of healing agent as function of hole size.**

a (mm)	t (mm)	Initial Stress (kPa)	$\delta_o$ (mm)	$\delta_i$ (mm)	$V_o$ (mm <sup>3</sup> )	$\Delta V$ (mm <sup>3</sup> )
0.08	1	0	0.0223	0.0259	0.016	0.0357
0.2	1	0	0.0327	0.0392	0.04	0.125
0.08	0.5	0	0.296	0.154	0.008	0.171
0.2	0.5	0	0.252	0.163	0.02	0.288
0.2	1	0.5	0.0292	0.0242	0.04	0.133
0.2	1	5	0.0588	0.0402	0.04	0.100

Again, an improvement in healing efficiency is shown with an increase in thickness. This is unsurprising, as the material loss and maximum deflection both decrease with increasing thickness. Increasing the initial pressure also improves the healing efficiency, with a decrease in the additional volume due to the decrease in material loss. However, all the cases show significant increase in material required, indicating that a microvascular system would be best suited for this application. Figures 9 and 10 below show typical deformations of the sealed cases.

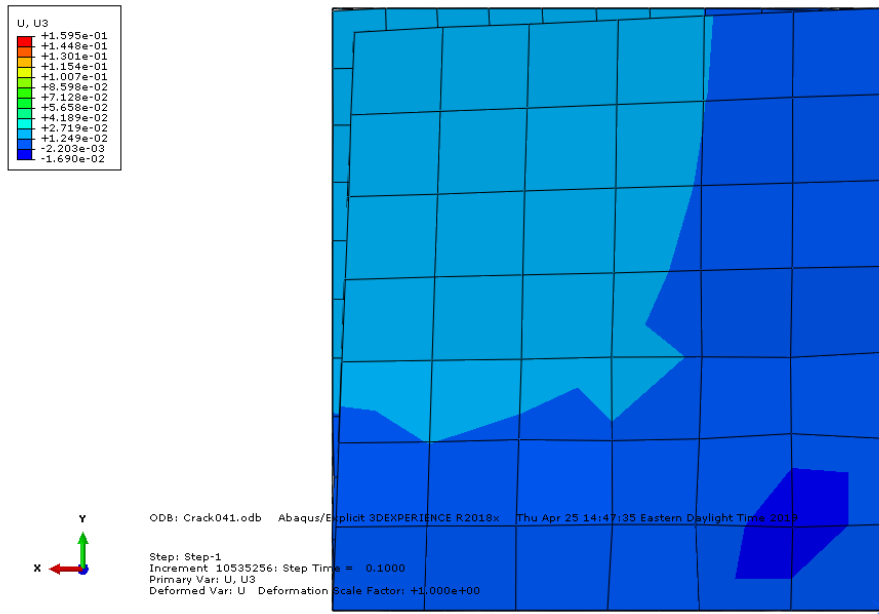


**Fig. 9 Bottom up view of deformations of sealed crack.**

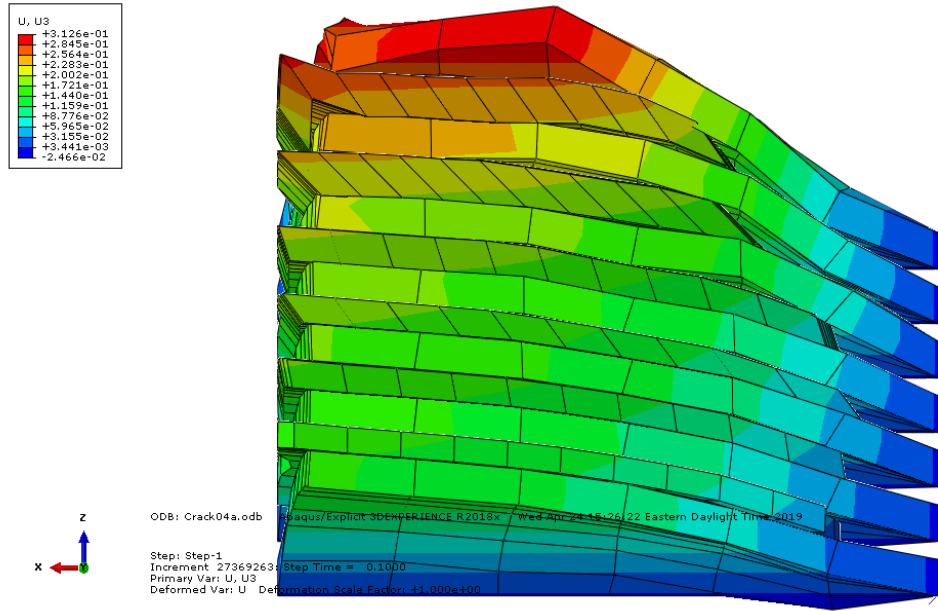


**Fig. 10 Side view of sealed crack.**

### C. Structural Strength

While the failure strength of the material cannot be analyzed via FEM, the increase in stress around the healed hole can be. Table 6 below lists the maximum stresses for each model, compares them to the stresses before damage.

**Table 6 Stress increase post healing**

a (mm)	t (mm)	Max Von Mises Stress, Pre-damage (MPa)	Max Von Mises Stress, Post-healing (MPa)	Stress Concentration Factor
0.08	1	0.478	1.624	3.40
0.2	1	0.478	1.648	3.45
0.08	0.5	0.812	2.387	2.94
0.2	0.5	0.812	2.35	2.89

While there is an increase in the maximum stress, with the peak stress (shown in Fig. 11) always occurring at the interface between the matrix and the cured healing agent, the maximum stress is always well below the yield stress of the polyurethane. Therefore, there does not need to be any significant concern over repeated failure of the material, assuming no additional forces.

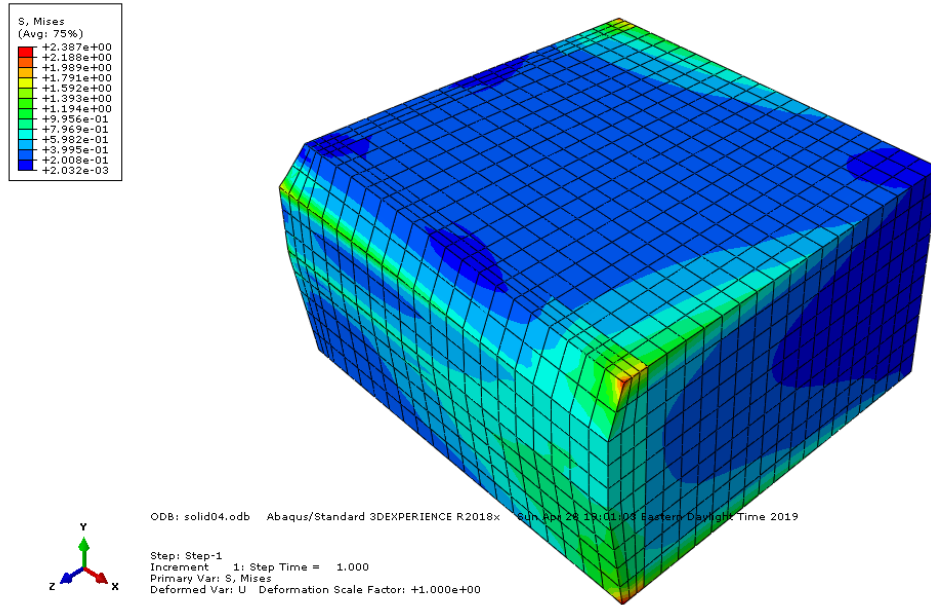


**Fig. 11 Von Mises stress in post-healing model.**

## VII. Discussion

Under the parameters considered in this study, the self-healing material was shown to heal microtears up to 0.2 mm wide. This level of healing would be useful for fracture and fatigue damages, such as from crazing or rubbing against a restraint system. It could also be used to repair a structure, either pre- or post-inflation, if the structure is left folded for an extended duration, such as a surface habitat being transported to Mars, and tears develop due to the crimping of the fabric or decreased ductility due to colder temperatures. While the stresses which develop post-healing are not large enough to induce failure under normal operating conditions, the local increase does increase the chance of repeated failure at the same location. However, any patch job on the material would likely result in the same phenomena, and, therefore, this risk needs minimal consideration. However, due to this risk and the large volume of healing material that is required, the microvascular system is recommended over the microencapsulation method, due to its ability to deliver additional material as needed and to effect repairs in the same location repeatedly. Another way to improve the reliability of the repair is to increase the thickness of the material. While this would increase the mass of the spacecraft, the additional healing capability may be worth the cost, depending on the risk of larger damages. Another possibility for increased efficiency is to increase the pressure under which the healing agent is kept. A higher pressure was shown to reduce the material loss during healing and improve the ability for the healing agent to repair the entire crack.

For this study, only a small segment of self-healing materials in a restricted set of scenarios were analyzed. This work could be extended to other types of self-healing, including any researched after this study was performed, and a wider variety of parameter changes, such as the viscosity or volume percentage of the healing agent. The other types of self-healing are more likely to affect the overall cost of the system, with the best system being determined by the application. For instance, a thermally activated system might perform well in areas where micrometeoroid impacts are the main concern, as the heat from the impact could trigger the healing process without requiring any additional energy input. The viscosity and volume percentage are expected to affect the healing efficiency of the system and, as no study was performed to choose the optimum values for these parameters, an improvement would almost certainly be found. The interaction between the bladder layer and its adjacent layers should also be analyzed, as this interaction would likely affect the results. However, without study, it cannot be predicted whether friction against the adjacent layers would slow the flow of the healing agent sufficiently to negate assistance from preventing material loss. The potential for outgassing of the healing agent should also be considered, and the effect the outgassing has on the healing process and efficiency should be evaluated. In addition, the effect of the self-healing on factors contributing to material failure other than the Von Mises stress. For instance, in fracture, it is possible that the self-healing could slow the crack growth, preventing catastrophic failure. Finally, physical tests should be conducted under the loading conditions

presented here to fully verify the results. While they have been compared to physical tests of similar cases for verification, and exact comparison should be performed to increase confidence both in these results and in the general method for application under more conditions.

### VIII. Conclusions

This study examined a variety of crack sizes, material thicknesses, and initial stresses to determine the suitability of self-healing materials for use in inflatable space structures. While only cracks of minimal widths, up to 0.2 mm, were found to successfully self-heal, adjusting parameters not examined in this study, such as viscosity, would likely help to improve the results of this study. These results show that self-healing materials do have promise for applications within inflatable structures, and, as research into self-healing materials improves, it's likely that the maximum healable crack size would increase.

### References

1. Cadogan, D., Scheir, C., Dixit, A., Ware, J., Cooper, E., and Kopf, P. "Intelligent Flexible Materials for Deployable Space Structures (InFlex)," *47th AIAA/ASME/ASCE/AHS/ASC Structures, Structural Dynamics, and Materials Conference*. American Institute of Aeronautics and Astronautics, 2006.
2. Jones, T. C. "Structural certification of human-rated inflatable space structures," *2018 IEEE Aerospace Conference*. 2018, pp. 1-13.
3. Brown, E., Sottos, N., and White, S. *Fracture Testing of a Self-Healing Polymer Composite*, 2002.
4. Wang, C., Liu, N., Allen, R., Tok, J. B.-H., Wu, Y., Zhang, F., Chen, Y., and Bao, Z. "A Rapid and Efficient Self-Healing Thermo-Reversible Elastomer Crosslinked with Graphene Oxide," *Advanced Materials* Vol. 25, No. 40, 2013, pp. 5785-5790.  
doi: doi:10.1002/adma.201302962
5. Alena, R., Ellis, S. R., Hieronymus, J., and Maclise, D. "Wireless Avionics and Human Interfaces for Inflatable Spacecraft," *2008 IEEE Aerospace Conference*. 2008, pp. 1-16.
6. Madaras, E. I., Anastasi, R. F., Seebo, J. P., Studor, G., McMakin, D. L., Nellums, R., and Winfree, W. P. "THE POTENTIAL FOR IMAGING IN SITU DAMAGE IN INFLATABLE SPACE STRUCTURES," *AIP Conference Proceedings* Vol. 975, No. 1, 2008, pp. 437-444.  
doi: 10.1063/1.2902693
7. Tan, W. C. K., Kiew, J. C., Siow, K. Y., Sim, Z. R., Poh, H. S., and Taufiq, M. D. "Self Healing of Epoxy Composite for Aircraft's Structural Applications," *Solid State Phenomena* Vol. 136, 2008, pp. 39-44.  
doi: 10.4028/www.scientific.net/SSP.136.39
8. Hager, M. D., Greil, P., Leyens, C., van Der Zwaag, S., and Schubert, U. S. "Self-healing materials," *Advanced materials (Deerfield Beach, Fla.)* Vol. 22, No. 47, 2010, pp. 5424-5430.  
doi: 10.1002/adma.201003036
9. Eichhorn, G. "Heating and vaporization during hypervelocity particle impact," *Planetary and Space Science* Vol. 26, No. 5, 1978, pp. 463-467.  
doi: [https://doi.org/10.1016/0032-0633\(78\)90067-3](https://doi.org/10.1016/0032-0633(78)90067-3)
10. Aïssa, B., Haddad, E., and Jamroz, W. *Self-healing Materials : Innovative Materials for Terrestrial and Space Applications*. Shrewsbury: Smithers Rapra, 2014.
11. Lampani, L., and Gaudenzi, P. "Numerical simulation of the behavior of inflatable structures for space," *Acta Astronautica* Vol. 67, No. 3, 2010, pp. 362-368.  
doi: <https://doi.org/10.1016/j.actaastro.2010.02.006>
12. White, S. R., Sottos, N. R., Geubelle, P. H., Moore, J. S., Kessler, M. R., Sriram, S. R., Brown, E. N., and Viswanathan, S. "Autonomic healing of polymer composites," *Nature* Vol. 409, 2001, p. 794.  
doi: 10.1038/35057232
13. Szmeczyk, T., Sienkiewicz, N., Woźniak, J., and Strzelec, K. *Polyurethanes as self-healing materials*, 2015.
14. Das, R., Melchior, C., and Karumbaiah, K. M. "11 - Self-healing composites for aerospace applications," *Advanced Composite Materials for Aerospace Engineering*. Woodhead Publishing, 2016, pp. 333-364.
15. "BASF Elastollan® 1185A Polyether Type Polyurethane Elastomer." MatWeb.
16. "Evonik VESTANAT® IPDI Polyisocyanate." MatWeb.
17. Chen, H., Tang, W., Ran, X., Zhang, M., and Xu, Z. "Measurement of the Mie-Grüneisen equation of state for polyimide," *Chinese Science Bulletin* Vol. 58, No. 6, 2013, pp. 585-588.  
doi: 10.1007/s11434-012-5602-4

18. NASA. "NASA-STD-3001, Volume 2, Revision A." 2015.
  19. Wijker, J. *Spacecraft Structures*: Springer, 2010.
  20. Beiermann, B. A., Keller, M. W., and Sottos, N. R. "Self-healing flexible laminates for resealing of puncture damage," *Smart Materials and Structures* Vol. 18, No. 8, 2009.
- doi: <https://doi.org/10.1088/0964-1726/18/8/085001>